Scanning electrochemical - ion conductance microscopy

DOI: 10.1002/anie.200((will be filled in by the editorial staff))

Multifunctional Nanoprobes for Nanoscale Chemical Imaging and Localized Chemical Delivery at Surfaces and Interfaces**

*Yasufumi Takahashi, Andrew I. Shevchuk, Pavel Novak, Yanjun Zhang, Neil Ebejer, Julie V. Macpherson, Patrick R. Unwin, Andrew J. Pollard, Debdulal Roy, Charles A. Clifford, Hitoshi Shiku, Tomokazu Matsue, David Klenerman, and Yuri E. Korchev**

The dynamics of chemical and biological processes at interfaces underpin a wide range of phenomena, from surface adsorption and crystal growth to signal transduction at the cell membrane. Since many interfaces have nanoscale structures which control these phenomena, it is vital to be able to perform measurements of chemical and biochemical fluxes on this length scale. One technique with the potential to measure chemically-specific fluxes on the nanoscale is scanning electrochemical microscopy (SECM),[1, 2] but a lack of reliable distance (feedback) control (in contrast to other scanning probe microscopes) and difficulties in fabricating small-scale electrodes have largely restricted the technique to the microscale.[3] Nanoscale electrochemical imaging has been demonstrated only rarely[4] and in rather unusual environments.[5, 6] There have been various attempts to introduce distance-control into SECM using, for example, shear force,[7-9] intermittent contact (IC)-SECM[10], SECM-AFM,[11-13] and the combination of SECM with scanning ion conductance microscopy (SICM).[14, 15] While these techniques have potential to open up nanoscale electrochemical imaging, they have the major disadvantage that they require specialist probes which are often difficult and time-consuming to fabricate and use.

Herein, we introduce an extremely quick (< 2 min) and simple process with a high success rate for making double-barrel carbon nanoprobes (DBCNPs) for use in SECM-SICM. The overall probe diameter is controllable on the nano- to microscale (*vide infra*), and the probes can be used for simultaneous chemical and topographical imaging, nano-positioning and localized chemical delivery and detection using SICM[16-19] distance feedback control. We first demonstrate their capability with approach curve measurements and by imaging test samples, and then by demonstrating their application to rat adrenal pheochromocytoma cells (PC12) by simultaneous high resolution imaging of the topography and electrochemical activity. Finally, exemplar studies of the localized chemical stimulation and detection of neurotransmitter release from PC12 cells using DBCNPs is reported which provides a platform for many future applications in cell biology.

DBCNPs are fabricated with one barrel filled with carbon for use as the SECM nanoelectrode, and the other barrel filled with electrolyte for SICM. The double barrel pipette is pulled from a "theta" quartz capillary (whose cross-section resembles the Greek capital letter theta, in which a straight septum divides the circular cross section into two isolated compartments). We have used this type of pipette previously (but with both barrels filled with electrolyte) for SICM and controlled deposition[20, 21] and for electrochemical imaging of electrode surfaces.[22] For SECM-SICM one barrel is coated internally with carbon, formed in-situ by the pyrolytic decomposition of butane;[23-25] the details of the fabrication method are described in the experimental section (Figure 1a). After carbon deposition, electrical contact is established by inserting a conductive wire through the top end of the pipette barrel into contact with the carbon layer. If the resulting conductive layer inside the barrel is sufficiently thick to fill and block the tip of that barrel, it provides an effective SECM electrode, where the exposed end of the conductive carbon is surrounded by the insulating quartz wall. Quartz glass provides a much more durable and high quality insulation layer than the polymer coatings used recently for SECM-SICM probes[14] that are prone to cracks and may contain pinholes leading to undesired leakage currents. The second barrel is

[*] Dr. Y. Takahashi, Dr. A. I. Shevchuk, Dr. P. Novak, Prof. Y. E. Korchev
Division of Medicine
Imperial College London
London W12 0NN (UK)
Fax: (+44)-208-383-8306
E-mail: y.korchev@ic.ac.uk

Prof. Yanjun Zhang
China National Academy of Nanotechnology & Engineering
Tianjin 300457 (China)
N. Ebejer, Prof. J. V. Macpherson, Prof. P. R. Unwin
Department of Chemistry
University of Warwick
Coventry CV4 7AL (UK)
Dr. A. J. Pollard, Dr. D. Roy, Dr. C. A. Clifford
National Physical Laboratory
Teddington TW11 0LW (UK)
Dr. H. Shiku, Prof. T. Matsue
Graduate School of Environmental Studies
Tohoku University
Aramaki Aoba 6-6-11-605, Sendai 980-8579, (Japan)
Advanced Institute of Materials Research
Tohoku University
Katahira, Aoba 2-1-1, Sendai 980-8577 (Japan)
Prof. David Klenerman
Department of Chemistry
Cambridge University
Cambridge,CB2 1EW (UK)

[**] This work was funded by the EPSRC and the Chemical and Biological Programme of the National Measurement System of the UK Department of Business, Innovation and Skills.. Y.T. acknowledges support from JSPS Postdoctoral Fellowships for Research Abroad. P.R.U. thanks the European Research Council for support.

Supporting information for this article is available on the WWW under http://www.angewandte.org or from the author.

unmodified, filled with electrolyte and used for SICM distance control and chemical delivery (Figure 1b).

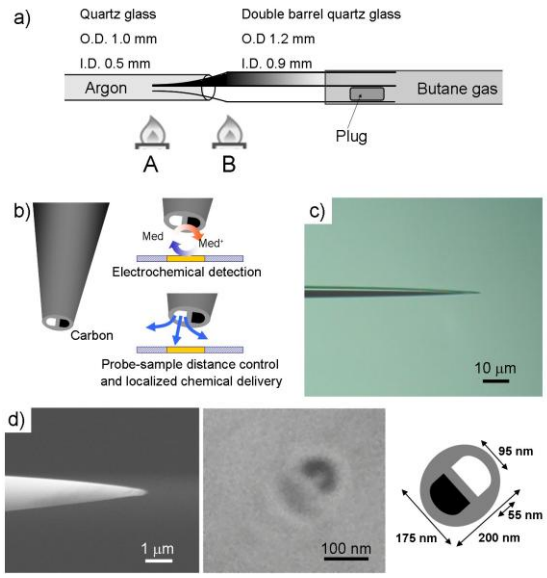

Figure 1. DBCNP fabricated using the pyrolytic carbon deposition method. a) Schematic illustration of the fabrication method of the DBCNP. b) The principle of combined SECM-SICM measurement with a DBCNP. c) Optical microscopy image of the side view of the DBCNP. d) FESEM images of the side and top of the DBCNP. Note, that carbon deposited inside one of the barrels appears lighter compared to an empty barrel on the FESEM image, but is shown black in the schematic representation (a,b).

The method allows fabrication of a wide range of DBCNP sizes from 20 nm to 2 µm. Examples of field emission scanning electron microscopy (FESEM) images of different-sized electrodes are presented in Figure 1 and S1. The sizes of DBCNP are controlled by the initial capillary pulling process and show high reproducibility; a typical size distribution of DBCNPs is shown in Figure S2. The supporting information also contains exemplar studies for voltammetry at these probes, for a range of apparent sizes and redox couples, from simple electron transfer to ferrocenylmethanol ($FcCH_2OH$) to fast scan cyclic voltammetry (FSCV) for the detection of dopamine (Figure S3).

Figure 1c and d show optical and FESEM images of the apex of a typical DBCNP. In this particular case the effective diameters of the SICM aperture and SECM carbon electrode are less than 100 nm and the overall probe diameter is just 200 nm, providing an important advantage for cell surface topographical and electrochemical imaging because the probe can access the cell surface and detect small roughness without unwanted probe-cell contact.[19]

Approach curves are considered to be one of the most effective ways to characterise the size (and shape) of SECM probes, where the diffusion-limited steady-state tip current for the detection of a bulk analyte is recorded as a function of tip-surface distance as the probe is translated towards a target surface.[26, 27] Figure 2a and b show typical experimental approach curves (black lines), for the SECM and SICM channels (recorded simultaneously), and fitted theoretical curves[4, 10, 26, 28] (red lines), for the translation of DBCNPs to both conductive and insulating substrates. As expected, the ion current signal decreases for both the insulating and conducting substrates, highlighting that it can be used for unambiguous distance feedback control.

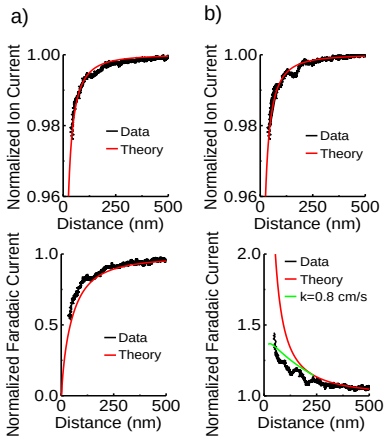

Figure 2. Approach curves of a DBCNP for simultaneous ion current (top) and electrochemical (bottom) measurements on an insulating (a), and conductive (b) substrate in 1.0 mM $FcCH_2OH$ + PBS. The SECM and SICM electrodes were held at 500 and 200 mV vs. reference Ag/AgCl electrode, respectively. The RG value used for the theoretical curves was 1.5.

The SECM approach for the insulating and conducting substrates showed negative (hindered diffusion) and positive (redox regeneration) feedback responses, respectively.[29] In this case, the electrode radius, *a*, was estimated to be 120 nm from the steady-state current in bulk solution and the fact that the negative feedback approach curve fits well to this value (and RG 1.5) indicates that the disks have a good planar geometry. Furthermore, it is noteworthy that by using the ion current feedback distance control, the electrode could approach the substrate as close as 50 nm without making direct contact. For the unbiased conductive surface, finite regeneration (surface redox) kinetics, with a heterogeneous rate constant, k = 0.80 cm/s, were observed because a small tip-substrate separation results in high mass transfer.[4, 10] Importantly, because the SICM channel provides the tip to surface distance, k is the only adjustable parameter in fitting the data. This highlights a key aspect of the SECM-SICM technique: the unambiguous quantitative determination of surface kinetics (and fluxes) because the distance between the tip and surface is known.

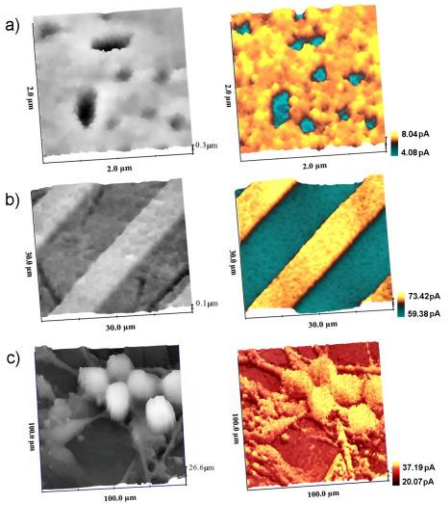

Figure 3. Simultaneous topographical (left) and electrochemical (right) images. a) PET in 1.0 mM $FcCH_2OH$ + PBS. b) Pt interdigitated array in 1.0 mM $FcCH_2OH$ and PBS. c) living sensory neurons in 0.5 mM $FcCH_2OH$ + HBSS. The SECM and SICM electrodes were held at 500 and 200 mV vs. reference Ag/AgCl electrode, respectively. Electrochemical images were based on an oxidation current of $FcCH_2OH$.

To evaluate the resolution of the DBCNP, we recorded topographical and electrochemical images of nanopores (pore diameters ~ 200 nm) in polyethylene terephthalate (PET) membranes. In our experiment, both sides of the membrane were filled with PBS containing 1.0 mM $FcCH_2OH$. The oxidation current of the $FcCH_2OH$ was recorded simultaneously with topography using a 28 nm radius carbon electrode in the DBCNP; the potentials of the SECM carbon and SICM Ag/AgCl electrodes were 500 and 200 mV, respectively, for this and other test substrates. A constant probe-sample separation of 30 nm was maintained by the SICM feedback. Figure 3a shows simultaneously recorded topographical and electrochemical images of the PET membrane where the pore shapes and the electrochemical signals corresponding with the pore positions were seen clearly. The decrease of the $FcCH_2OH$ oxidation current indicates that the diffusion of the $FcCH_2OH$ was blocked by the pore (decreased SECM channel current), because the probe moves towards membrane under SICM feedback control as the probe encounters the pore.

To test the DBCNPs further, SECM-SICM was used to image a Pt interdigitated array electrode (IDA) (Figure 3b). A constant probe-sample separation of 100 nm was maintained by the SICM feedback, so that the SECM current clearly reflects the electrochemical activity of the sample. The oxidation current of the $FcCH_2OH$ was recorded simultaneously with the topography using a DBCNP (88 nm radius carbon electrode). It is clear that the electrochemical signal increases over the Pt bands (100 nm high in the SICM topography image) due to redox cycling, as for the approach curves in Figure 2c. Importantly, with this design of SECM-SICM probe, the insulation is considerably better (there are no pinholes or recessing of the electrode) and the probe size is smaller than previous report.[14]

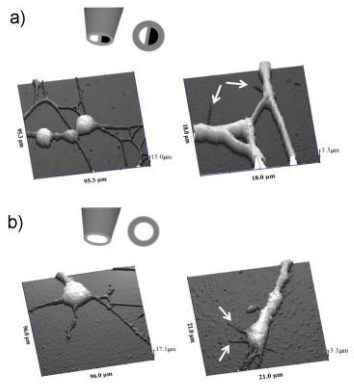

Figure 4. Nanoscale topography images of differentiated PC12 cells using (a) the DBCNP and (b) a single SICM nanopipette. The arrows showed the dendritic structures.

To demonstrate electrochemical and topographical imaging of neurons using DBCNPs (240 nm radius carbon electrode), we visualized the permeation of $FcCH_2OH$, a hydrophobic mediator which can cross the cell membrane, simultaneously with the topography of living sensory neurons. Figure 3c shows the SECM-SICM images of sensory neurons in Hank's buffered salt solution (HBSS) containing 0.5 mM $FcCH_2OH$. The tall cell bodies, exceeding 25 μm in height, and dendritic structures are clearly observed in both the SICM and SECM images, which correlate very well. The SICM images represent the topography, whereas the SECM images measure the flux of $FcCH_2OH$. When the probe is over the bare petri dish, a current of 23 pA is typically recorded, which is the value expected for hindered diffusion. In contrast, when the probe is over the cells, an enhanced current is observed which approaches the value of 38 pA when the probe is in bulk solution. This indicates that the cellular membrane is permeable to $FcCH_2OH$ and that the permeability can be visualized, largely free from topographical effects, due to the independent distance control from SICM. Furthermore, note that the electrochemical response shows no deterioration in this biological medium. Thus, the DBCNP can be used for localized electrochemical measurements and simultaneous surface topography imaging of complex live biological samples.

To further validate the capabilities of SECM-SICM for imaging living cell topography we compared the topography of differentiated PC12 cells using both a DBCNP and a single SICM nanopipette (Figure 4a and 4b respectively). The diameters of the SICM aperture of the DBCNP and the SICM nanopipette were both 100 nm. The qualities of the topographic images were comparable: similar dendritic structures, less than 200 nm diameter, were observed on both images (Figure 4a and b, white arrows).

To enhance electrochemical detection sensitivity of the DBCNPs for detecting the neurotransmitter release it is important to increase the carbon surface area, but not the SICM barrel aperture for distance feedback control. We thus fabricated cylindrical-shaped DBCNPs by depositing additional carbon on the outside of the pipette. The method for depositing carbon on the outer surface of the micropipette tip was as described previously,[25] such that the steady-state current measured in 1 mM $FcCH_2OH$ and PBS was 1.85 nA. We then measured the neurotransmitter release from undifferentiated PC12 cells using this type of probe (Figure 5a). A key advantage of the DBCNP is that it can be positioned with very high precision using the SICM control: in the present studies it was positioned 500 nm above a PC12 cell.

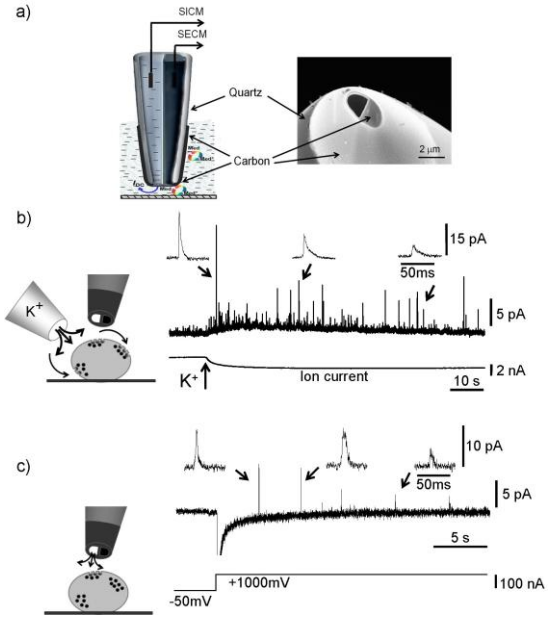

Figure 5. Detection of the release of the neurotransmitter using the cylindrical-shaped DBCNP. a) SEM image of a cylindrical-shaped DBCNP. A series of current spikes corresponding to neurotransmitter release detected after (b) whole cell stimulation of 105 mM K^+ using another micropipette and (c) voltage-driven K^+ delivery using a DBCNP. The carbon electrode was held at 650 mV vs. reference Ag/AgCl electrode.

To stimulate neurotransmitter release, we depolarized a PC12 cell by whole cell stimulation of 105 mM K^+ using another micropipette (a = 3 μm). Figure 5b shows a series of current spikes

corresponding to neurotransmitter release detected at the probe. The insets of Figure 5b shows expanded views of the releasing signal where the amplitudes and the widths of the spike are clearly visible. It was shown previously that the amplitude and the shape of the signal was dependent on the separation between the electrode and release site.[30] It is also possible to observe the increase in local K^+ concentration at the DBCNP via the increase of negative ion current (Figure 5b, bottom trace).

One of the great advantages of using DBCNPs is that the barrel filled with electrolyte can be used for application of different reagents for local stimulation of the cell: the voltage-driven local chemical change produced by nanopipette is effective to control the biological sample function.[31] Therefore, in the next series of experiments we performed voltage-driven K^+ application using the DBCNP itself to achieve both local depolarization of the cell membrane and simultaneous neurotransmitter detection. With the SICM barrel filled with 3 M KCl, the SICM electrode applied voltage was changed from -50 mV to 1000 mV, to eject potassium ions from the SICM barrel pipette towards the cell surface inducing local triggering of neurotransmitter release. Figure 5c shows a series of current spikes, detected after local stimulation with the voltage-driven K^+ application.

With local stimulation we always detected either a low frequency of current spikes or no spikes at all compared with whole cell stimulation. This suggests that the DBCNP can be used to induce and detect localized neurotransmitter release over the cell surface opening up possibilities to perform the mapping of neurotransmitter release sites.

We have developed a simple, affordable and quick method of fabricating a DBCNP for functional nanoscale (electro)chemical imaging using SICM distance feedback control. The fabrication method yields probes with controllable diameters in the range 20 nm to 2 μm with excellent temporal and spatial resolution. Among many possibilities in the physical and life sciences, this novel probe allows the mapping of sites of neurotransmitter release together with the associated changes in the cell topography, that occur during exocytosis, and in the future this technique could be extended to performing intracellular measurements. The capability to produce nanoscale electrodes with integrated distance control in a simple fashion allows true nanoscale SECM (chemical flux) imaging with widespread applications.

Experimental Section

For fabrication of the DBCNP, a quartz theta glass capillary (O.D. 1.2mm, I.D. 0.9 mm; Sutter Instrument, USA) was pulled using a CO_2 laser puller (model P-2000, Sutter Instrument, San Rafael, CA, USA). Figure 1a shows a schematic illustration of the fabrication system. Butane was passed through the quartz capillary via Tygon tube (O.D. 2.4 mm, I.D. 0.8 mm). First, both of the ends of the barrels were blocked with Blu-tack. Next, one of the barrels was opened and pressurized with butane gas in order to deposit carbon inside this barrel only. The other barrel remained blocked and therefore no carbon was deposited so it could be used for SICM. The taper of the pipette was inserted into another quartz capillary (O.D. 1.0 mm, I.D. 0.7 mm; Sutter Instrument, USA) which was filled with argon gas to prevent oxidation of the carbon layer and bending of the capillary by high temperature. This approach also protected the pipette aperture from closing due to the softening of the quartz pipette walls. To form pyrolytic carbon layer inside the capillary the pipette taper was then heated with a Bunsen burner for times ranging from 0.5 s for a 100 nm radius electrode through to 3 s for a 1 μm radius electrode. The deposited layer of carbon inside the pipette is clearly observed in the SEM image of a cross-section of a DBCNP shown in Figure S1c. The amount of deposited carbon was proportional to the heat delivered and heating time. However, overheating by supplying too high a temperature or by prolonged heating time resulted in pipette aperture collapse, reducing the effective surface area of carbon exposed. It was found that when the electrochemical signal was too small, the time taken to heat the taper had been too long.

To detect neurotransmitter release from a PC12 cell, increasing the carbon surface area is required for enhanced sensitivity of the electrochemical measurement. We therefore fabricated cylindrical-shaped DBCNPs by depositing carbon on the outside of the top of the tip. Details of the deposition have been described in a previous report.[25] The argon flow (1.2 L/min) is important to control the outside carbon deposition area. Additionally, the activation of the carbon electrode was also an important process for the detection of neurotransmitters.[32] The DBCNPs were activated by applying -1.0 V vs. reference Ag/AgCl electrode for 1 min.

The DBCNP was difficult to fill with the electrolyte solution due to air plugs that formed close to the pipette taper. To force these air bubbles out of the electrolyte, we used a cigarette gas lighter to quickly heat the solution inside the pipette. The heat supplied by the gas lighter was not great enough to soften the quartz walls of the pipette but resulted in rapid air bubble expansion and movement towards the wider part of the pipette unblocking the pipette tip. This allowed reliable filling of the pipette with electrolyte.

Ferrocenylmethanol ($FcCH_2OH$; Sigma-Aldrich), hexaammineruthenium (III) chloride ($Ru(NH_3)_6Cl_3$; Sigma-Aldrich), Hank's buffered salt solution (HBSS; Invitrogen) were purchased and used as received. PBS was prepared from 7.2 mM Na_2HPO_4 $12H_2O$, 2.8 mM KH_2PO_4, and 150 mM NaCl (pH 7.4). PET membranes were kindly provided by Dr. Pavel Apel (Flerov Laboratory of Nuclear Reactions, Joint Institute for Nuclear Research, Russia).

Sensory neurons were kindly provided by Dr. Guy Moss. PC12 cells were purchased from Health Protection Agency Culture Collections, UK. Cells were kept in a growth medium consisting of an RPMI-1640 (GIBCO) supplemented with 10% heat-inactivated horse serum (GIBCO), 5 % fetal calf serum (GIBCO), 100 μg/ml streptomycin and 100 U/ml penicillin (GIBCO). The nerve growth factor (50 ng/ml, 2.5 S; GIBCO) was added to the medium for sensory neurons and differentiation to the neuronal PC12. Cells were maintained at 37 ℃ in an atmosphere of humidified air with 95% O_2/5% CO_2. The detail of the differentiation to the neuronal PC12 has been described previously.[8]

The SECM-SICM instrument used was similar to one previously described[14] and operated in hopping mode.[19] The currents were measured with a dual channel MultiClamp700B patch–clamp amplifier (Axon Instruments). The electrochemical and ion current signals were filtered using low-pass filter at 1 kHz. The data were digitized and analyzed with continuous data acquisition hardware and software (Axon Digidata 1322A, Axon Instruments). The set point for SICM imaging was 0.4-1.0 % of I_{REF}.

The probe position was controlled by a XY and Z piezoelectric scanner (Physik Instrumente, 621.2CL and 621.ZCL), using an amplifier module (Physik Instrumente, E-503.00) and servo control module (Physik Instrumente, E-509.C3). The system was controlled by a program written in Delphi (Borland) and Code

Composer Studio (Texas Instruments, USA) for a ScanIC controller (Ionscope, UK).

Received: ((will be filled in by the editorial staff))
Published online on ((will be filled in by the editorial staff))

Keywords: scanning electrochemical microscopy · scanning ion conductance microscopy · nanoelectrode · neurotransmitter detection · living cell imaging

[1] A. Schulte, W. Schuhmann, *Angew. Chem. Int. Ed.* **2007**, *46*, 8760.
[2] G. Wittstock, M. Burchardt, S. E. Pust, Y. Shen, C. Zhao, *Angew. Chem. Int. Ed.* **2007**, *46*, 1584.
[3] S. Amemiya, A. J. Bard, F. R. F. Fan, M. V. Mirkin, P. R. Unwin, *Annual Review of Analytical Chemistry* **2008**, *1*, 95.
[4] F. O. Laforge, J. Velmurugan, Y. X. Wang, M. V. Mirkin, *Anal. Chem.* **2009**, *81*, 3143.
[5] F. R. F. Fan, A. J. Bard, *Proc. Natl. Acad. Sci. U. S. A.* **1999**, *96*, 14222.
[6] J. V. Macpherson, P. R. Unwin, *Anal. Chem.* **2000**, *72*, 276.
[7] A. Hengstenberg, A. Blochl, I. D. Dietzel, W. Schuhmann, *Angew. Chem. Int. Ed.* **2001**, *40*, 905.
[8] Y. Takahashi, Y. Hirano, T. Yasukawa, H. Shiku, H. Yamada, T. Matsue, *Langmuir* **2006**, *22*, 10299.
[9] Y. Takahashi, T. Miyamoto, H. Shiku, R. Asano, T. Yasukawa, I. Kumagai, T. Matsue, *Anal. Chem.* **2009**, *81*, 2785.
[10] K. McKelvey, M. A. Edwards, P. R. Unwin, *Anal. Chem.* **2010**, *82*, 6334.
[11] D. P. Burt, N. R. Wilson, J. M. R. Weaver, P. S. Dobson, J. V. Macpherson, *Nano Lett.* **2005**, *5*, 639.
[12] C. E. Gardner, P. R. Unwin, J. V. Macpherson, *Electrochem. Commun.* **2005**, *7*, 612.
[13] A. Ueda, O. Niwa, K. Maruyama, Y. Shindo, K. Oka, K. Suzuki, *Angew. Chem. Int. Ed.* **2007**, *46*, 8238.
[14] Y. Takahashi, A. I. Shevchuk, P. Novak, Y. Murakami, H. Shiku, Y. E. Korchev, T. Matsue, *J. Am. Chem. Soc.* **2010**, *132*, 10118.
[15] D. J. Comstock, J. W. Elam, M. J. Pellin, M. C. Hersam, *Anal. Chem.* **2010**, *82*, 1270.
[16] P. K. Hansma, B. Drake, O. Marti, S. A. C. Gould, C. B. Prater, *Science* **1989**, *243*, 641.
[17] Y. E. Korchev, C. L. Bashford, M. Milovanovic, I. Vodyanoy, M. J. Lab, *Biophys. J.* **1997**, *73*, 653.
[18] A. I. Shevchuik, G. I. Frolenkov, D. Sanchez, P. S. James, N. Freedman, M. J. Lab, R. Jones, D. Klenerman, Y. E. Korchev, *Angew. Chem. Int. Ed.* **2006**, *45*, 2212.
[19] P. Novak, C. Li, A. I. Shevchuk, R. Stepanyan, M. Caldwell, S. Hughes, T. G. Smart, J. Gorelik, V. P. Ostanin, M. J. Lab, G. W. Moss, G. I. Frolenkov, D. Klenerman, Y. E. Korchev, *Nat. Methods* **2009**, *6*, 279.
[20] K. T. Rodolfa, A. Bruckbauer, D. J. Zhou, Y. E. Korchev, D. Klenerman, *Angew. Chem. Int. Ed.* **2005**, *44*, 6854.
[21] K. T. Rodolfa, A. Bruckbauer, D. J. Zhou, A. I. Schevchuk, Y. E. Korchev, D. Klenerman, *Nano Lett.* **2006**, *6*, 252.
[22] N. Ebejer, M. Schnippering, A. W. Colburn, M. A. Edwards, P. R. Unwin, *Anal. Chem.* **2010**, *82*, 9141.
[23] Y. T. Kim, D. M. Scarnulis, A. G. Ewing, *Anal. Chem.* **1986**, *58*, 1782.
[24] D. K. Y. Wong, L. Y. F. Xu, *Anal. Chem.* **1995**, *67*, 4086.
[25] M. McNally, D. K. Y. Wong, *Anal. Chem.* **2001**, *73*, 4793.
[26] J. L. Amphlett, G. Denuault, *J. Phys. Chem. B* **1998**, *102*, 9946.
[27] Y. H. Shao, M. V. Mirkin, *J. Phys. Chem. B* **1998**, *102*, 9915.
[28] M. A. Edwards, C. G. Williams, A. L. Whitworth, P. R. Unwin, *Anal. Chem.* **2009**, *81*, 4482.
[29] J. Kwak, A. J. Bard, *Anal. Chem.* **1989**, *61*, 1794.
[30] R. M. Wightman, T. J. Schroeder, J. M. Finnegan, E. L. Ciolkowski, K. Pihel, *Biophys. J.* **1995**, *68*, 383.
[31] J. D. Piper, C. Li, C. J. Lo, R. Berry, Y. Korchev, L. M. Ying, D. Klenerman, *J. Am. Chem. Soc.* **2008**, *130*, 10386.
[32] F. G. Gonon, C. M. Fombarlet, M. J. Buda, J. F. Pujol, *Anal. Chem.* **1981**, *53*, 1386.

Entry for the Table of Contents (Please choose one layout)

Layout 1:

Scanning electrochemical - ion conductance microscopy

Yasufumi Takahashi, Andrew I. Shevchuk, Pavel Novak, Yanjun Zhang, Neil Ebejer, Julie V. Macpherson, Patrick R. Unwin, Andrew J. Pollard, Debdulal Roy, Charles A. Clifford, Hitoshi Shiku, Tomokazu Matsue, David Klenerman, and Yuri E. Korchev*

_____ **Page – Page**

Multifunctional Nanoprobes for Nanoscale Chemical Imaging and Localized Chemical Delivery at Surfaces and Interfaces

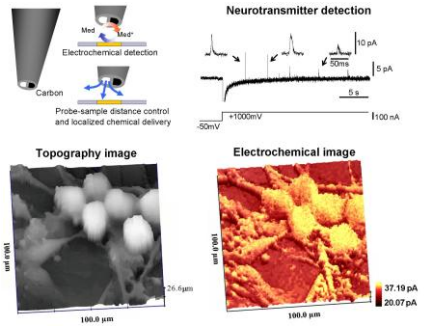

A multifunctional carbon nanoelectrode: A new and simple method of producing double-barrel carbon nanoprobes with integrated distance control for simultaneous nanoscale electrochemical and ion conductance microscopy is introduced. The fabrication method takes less than two minutes, and controllably produces a wide range of probe sizes. The nanoprobes allow simultaneous non-contact topographical and electrochemical imaging of living neurons, as well as localized K^+ delivery and simultaneous neurotransmitter detection.